Compressed Channel Estimation With Position-Based ICI Elimination for High-Mobility SIMO-OFDM Systems

Xiang Ren, Meixia Tao, *Senior Member, IEEE*, and Wen Chen, *Senior Member, IEEE*

***Abstract*—Orthogonal frequency-division multiplexing (OFDM) is widely adopted for providing reliable and high-data-rate communication in high-speed train (HST) systems. However, with increasing train mobility, the resulting large Doppler shift introduces intercarrier interference (ICI) in OFDM systems and greatly degrades channel estimation accuracy. Therefore, it is necessary and important to investigate reliable channel estimation and ICI mitigation methods in high-mobility environments. In this paper, we consider a typical HST communication system and show that the ICI caused by large Doppler shifts can be mitigated by exploiting the train position information and the sparsity of the basis expansion model (BEM)-based channel model. Then, we show that for the complex-exponential BEM (CE-BEM)-based channel model, the ICI can be completely eliminated to get the ICI-free pilots at each receive antenna. After that, we propose a new pilot pattern design algorithm to reduce system coherence to improve the compressed-sensing-based channel estimation accuracy. The proposed optimal pilot pattern is independent of the number of receive antennas, the Doppler shifts, train position, or train speed. Simulation results confirm the effectiveness of the proposed scheme in high-mobility environments. The results also show that the proposed scheme is robust to the speed of the moving train.**

***Index Terms*—Channel estimation, compressed sensing (CS), high mobility, intercarrier interference (ICI), orthogonal frequency-division multiplexing (OFDM), single-input multiple-output (SIMO).**

I. Introduction

HIGH-speed trains (HSTs) have been increasingly developed in many countries and have made a particularly great impact in China. There is a growing demand of offering passengers the data-rich wireless communications with high data rate and high reliability. Orthogonal frequency-division multiplexing (OFDM), as a leading technique in the current Long-Term Evolution (LTE) and future evolution of cellular networks, have demonstrated great promise in achieving high data rate in stationary and low-mobility environments. In the HST environment, however, since the train travels at a speed of more than 350 km/h, the high Doppler shift destroys the orthogonality, resulting in intercarrier interference (ICI) in OFDM systems. This directly degrades channel estimation accuracy and significantly affects overall system performance. It is thus necessary and important to investigate reliable channel estimation and ICI mitigation methods in high-mobility environments.

Channel estimation in OFDM systems over time-varying channels has been a long-standing issue [1]–[11]. The existing works can be generally divided into three categories based on the channel model properties they adopted. The first category of estimation methods adopted the linear time-varying channel model, i.e., the channel varies with time linearly in one or more OFDM symbols, such as [1] and [2]. The second category employs the basis expansion model (BEM) such as [3] and [4]. Note that both these two channel models implicitly assume that the channel is in rich-scattering environment with a sufficient multipath. The third category of channel estimation methods is based on the recent research finding that wireless channels tend to exhibit sparsity, where the channel properties are dominated by a relatively small number of dominant channel coefficients. To utilize the channel sparsity, several works [5]–[11] studied the applications of compressed sensing (CS) in the channel estimation. In [5]–[10], channel sparsity was introduced, and several CS-based estimation methods were proposed, which, however, did not consider the effect of a large Doppler shift. In the presence of a large Doppler shift, Taubock *et al.* [11] indicated that the channel sparsity is notably reduced, and the pilots suffer from the strong ICI introduced by the data, yielding poor estimation performance. To address these two problems, in [11], a BEM optimization method was proposed to enhance the channel sparsity, and an iterative CS-based channel estimator with the random pilot pattern to reduce the ICI was designed. However, the iterative procedure incurs high computational complexity and results in error propagation.

Another line of research to improve the performance of channel estimation is to consider the pilot design and channel estimation jointly. Recently, many studies considered this problem based on the CS-based channel estimation methods. Coherence is a critical metric in CS as it directly influences the CS recovery performance [12]–[14]. In [12] and [13], it was concluded that lower system coherence leads to a better recovery performance.

Manuscript received January 27, 2015; revised June 21, 2015; accepted August 2, 2015. Date of publication August 20, 2015; date of current version August 11, 2016. This work was supported in part by the National 973 Project under Grant 2012CB316106, by the Natural National Science Foundation of China under Grant 61322102 and Grant 61221001, and by the Southeast University National Key Laboratory on Mobile Communications under Grant 2013D11. The review of this paper was coordinated by Prof. X. Wang.

X. Ren and M. Tao are with the Department of Electronic Engineering, Shanghai Jiao Tong University, Shanghai 200240, China (e-mail: renx@sjtu.edu.cn; mxtao@sjtu.edu.cn).

W. Chen is with the Department of Electronic Engineering, Shanghai Jiao Tong University, Shanghai 200240, China, and also with the School of Electronic Engineering and Automatic, Guilin University of Electronic Technology, Guilin 541004, China (e-mail: wenchen@sjtu.edu.cn).

Color versions of one or more of the figures in this paper are available online at http://ieeexplore.ieee.org.

Digital Object Identifier 10.1109/TVT.2015.2471085

Based on these results, previous works [15]–[19] proposed several pilot design methods to reduce the system coherence for single-input–single-output (SISO)/multiple-input–multiple-output (MIMO) OFDM systems and hence to improve the CS-based channel estimation performance. In our previous work [18], we proposed a position-based joint pilot pattern and pilot symbol design method for high-mobility OFDM systems, where different pilots are designed for the Doppler shifts at different train positions and then stored into a codebook. For each train position, the system selects the corresponding optimal pilot and uses it to estimate the channel.

In the presence of a high Doppler shift, the resulting ICI attenuates the desired signal and reduces the effective signal-to-noise ratio (SNR) in OFDM reception, resulting in degraded system performance. To combat the ICI effect, several techniques have been proposed [15]–[22]. In [15]–[17], the ICI was considered Gaussian noise, which needs low complexity, but its performance degraded quickly with large Doppler shift. In [18] and [20], ICI mitigation methods based on an iterative process were proposed. These methods are effective for the mitigation of ICI but incur high computational complexity and result in error propagation. In addition, in [19], a pilot pattern design method with the ICI-free structure was designed for the distributed CS (DCS)-based channel estimator. This method, however, needs a large number of pilots to eliminate the ICI, which highly reduces the spectral efficiency. In [21] and [22], joint carrier frequency offset and channel estimation methods were proposed to compensate the induced ICI.

This paper is based upon our previous work [18] with the aim of improving the channel estimation performance by taking ICI into account. Similar to [18], we consider an HST communication system where the instantaneous position and speed of the moving train can be estimated, e.g., using a GPS. However, different from [18], we consider the single-input–multiple-output (SIMO) scenario. Note that the method in [18] cannot be directly applied to SIMO systems. The optimal pilot proposed in [18] for the SISO system is different for different train positions. When it is applied in the SIMO system, different optimal pilots need to be sent for different receive antennas due to their different positions. This will certainly reduce the spectral efficiency.

In this paper, based on the conventional BEM, we first show that the ICI caused by the large Doppler shift can be mitigated by exploiting the train position information. The relationships between the dominant channel model, the dominant channel coefficients, the Doppler shift, and the train position are also given. Then, considering the complex-exponential BEM (CE-BEM), we propose a new low-complexity position-based ICI elimination method, by which we can get the ICI-free pilots at each receive antenna. In contrast to the iterative ICI mitigation methods in [11], [18], and [20], which incur high computational complexity under a large Doppler shift, the proposed method only requires a permutation of the received subcarriers with much less complexity. In addition, different from the methods in [4] and [19], needing a large number of guard pilots to eliminate the ICI, the proposed method does not need a guard pilot, which highly improves the spectral efficiency as well. After getting the ICI-free pilots, we formulate the pilot pattern design problem to minimize the system average coherence and propose a new pilot design algorithm to solve it. In particular, the optimal pilot pattern is independent of the train speed, the train position, the Doppler shift, or the number of receive antennas. Thus, the system only needs to store one pilot pattern, which highly reduces the system complexity in contrast to [18] that selects different pilots for different train positions. In addition, different from the methods in [18] and [20] that the channel estimation performances are highly influenced by the system mobility, simulation results demonstrate that the proposed scheme is robust to the high mobility.

The remainder of this paper is organized as follows. Section II introduces the HST communication system, the SIMO-OFDM system model, and the BEM channel model. In Section III, we exploit the position information of the BEM. Then, for the CE-BEM, we introduce a new position-based ICI elimination method. In Section IV, after briefly review some CS fundamentals, we formulate the pilot design problem and propose a new low coherence pilot pattern design algorithm. The complexity and the practical applicability of the proposed scheme is also discussed. Section V presents simulation results in the high-mobility environment. Finally, Section VI concludes this paper.

Notations: $\|\cdot\|_{\ell_0}$ denotes the number of nonzero entries in a matrix or vector, and $\|\cdot\|_{\ell_2}$ is the Euclidean norm. $\mathbf{X}(\mathbf{w},:)$ denotes the rows of matrix $\mathbf{X}$ whose row indexes are in vector $\mathbf{w}$. The superscripts $(\cdot)^T$ and $(\cdot)^H$ denote the transposition and Hermitian of a matrix, respectively. $\lceil\cdot\rceil$ denotes the round up operator, $\lfloor\cdot\rfloor$ denotes the round down operator, $\otimes$ denotes the Kronecker product, and $\mathrm{diag}\{\cdot\}$ denotes the operator that changes a vector to a diagonal matrix. $\mathbf{0}$ denotes the all-zero matrix, $\mathbf{I}_K$ denotes the $K \times K$ identity matrix, and $\mathbf{I}_K^{\langle q\rangle}$ denotes a permutation matrix, which is obtained from $\mathbf{I}_K$ by shifting its column circularly $|q|$ times to the right for $q < 0$ and to the left otherwise. Finally, $\mathbb{C}^{M\times N}$ denotes the set of $M \times N$ matrices in the complex field, and $\mathbb{R}$ denotes the real field.

II. System Model

A. HST Communication System

We consider a typical broadband wireless communication system for high-speed trains (HSTs) [18], [23], as shown in Fig. 1. The communication between the base stations (BSs) and the mobile users is conducted in a two-hop manner through a relay station (RS) deployed on the train. The RS is connected with several antennas evenly located on the top of the train to communicate with the BS. Moreover, the RS is also connected with multiple indoor antennas distributed in the train carriages to communicate with mobile users by existing wireless communication technologies. The BSs are located along the railway at some intervals and connected with optical fibers. Here, we assume that each BS is equipped with one antenna for simplicity and has the same transmit power and coverage range. Similar to [18], we assume that the HST is equipped with a GPS that can estimate the HST's instant position and speed information perfectly and send them to the RS with no time delay [24]. However, different from [18], in this paper, the BS does not need to receive these information from the GPS.

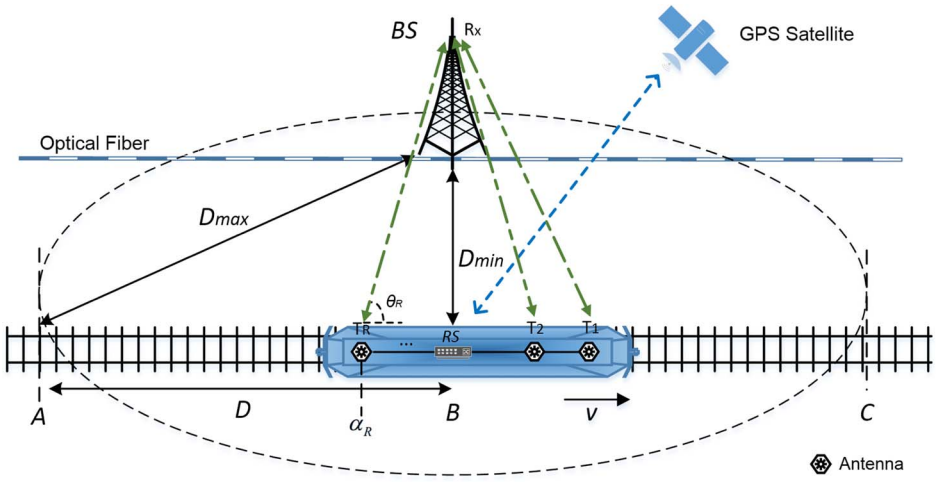

Fig. 1. Structure of a SIMO HST communication system.

In Fig. 1, we assume that the HST is traveling toward a fixed direction at a constant speed v. Let $D_{\max}$ denote the maximum distance from the BS to the railway (i.e., the position A and C to BS), $D_{\min}$ denote the minimum distance (i.e., the position B to BS), and D denote the distance between A and B. The R receive antennas evenly located on the top of the HST are denoted $\{T_r\}_{r=1}^{R}$, and R_x denotes the antenna equipped on the BS. In each cell, we define α_r as the distance between the rth receive antenna and the position A and define θ_r as the angle between the BS to T_r and the railway. When the HST moves from A to C, θ_r changes from $\theta_{\min}$ to $\theta_{\max}$. If $D_{\max} \gg D_{\min}$, we have $\theta_{\min} \approx 0^\circ$ and $\theta_{\max} \approx 180^\circ$. For T_r at a certain position α_r, with the carrier frequency f_c and the light speed c, it suffers from a Doppler shift $f_r = (v/c) \cdot f_c \cos\theta_r$, where θ_r can be calculated from α_r (supported by the GPS), and v is provisioned by the position tracking.[1] In addition, we assume that f_r is constant within one OFDM symbol.

B. SIMO-OFDM System

In this paper, we only consider the first-hop communication in the HST system, i.e., the communication from the BS to the RS. It is treated as a SIMO-OFDM system with one transmit antenna and R receive antennas. Suppose there are K subcarriers. The transmit signal at the kth subcarrier during the nth OFDM symbol is denoted $X^n(k)$, for $n = 0, 1, \ldots, N-1$ and $k = 0, 1, \ldots, K-1$. At the BS, after passing the inverse discrete Fourier transform (DFT) and inserting the cyclic prefix (CP), the signals are transmitted to the wireless channel. At the rth receive antenna, after removing the CP and passing the DFT operator, the received signal in the frequency domain is represented as

$$\mathbf{y}_r^n = \mathbf{F}\tilde{\mathbf{H}}_r^n\mathbf{F}^H\mathbf{x}^n + \mathbf{n}_r^n \quad (1)$$

$$= \mathbf{H}_r^n\mathbf{x}^n + \mathbf{n}_r^n \quad (2)$$

[1]Note that the GPS is widely considered in current HST systems [23], [24]. For some environments where the GPS is not available, some carrier frequency offset estimation methods in [21] and [22] can be utilized to estimate the Doppler shift.

where $\mathbf{y}_r^n = [Y_r^n(0), Y_r^n(1), \ldots, Y_r^n(K-1)]^T$ is the received signal vector over all subcarriers during the nth OFDM symbol; $\tilde{\mathbf{H}}_r^n$ denotes the time-domain channel matrix between the transmit antenna and the rth receive antenna; $\mathbf{H}_r^n \triangleq \mathbf{F}\tilde{\mathbf{H}}_r^n\mathbf{F}^H$ denotes the channel matrix in the frequency domain; $\mathbf{F}$ is the $K \times K$ DFT matrix; $\mathbf{x}^n = [X^n(0), X^n(1), \ldots, X^n(K-1)]^T$ is the transmitted signal vector; $\mathbf{n}_r^n = [N_r^n(0), N_r^n(1), \ldots, N_r^n(K-1)]^T$ denotes the noise vector; and $N_r^n(k)$ is the additive white Gaussian noise with a zero mean and σ_ε^2 variance. Let $h_r^n(k,l)$ denote the lth $(0 \le l \le L-1)$ channel tap at the kth time instant within the nth OFDM symbol between the transmit antenna and the rth receive antenna. In particular, $\tilde{\mathbf{H}}_r^n$ takes a pseudo-circulant form as [3]

$$\tilde{\mathbf{H}}_r^n(k,d) = h_r^n\left(k, |k-d|_K\right), \quad k,d \in [0, K-1] \quad (3)$$

where $\tilde{\mathbf{H}}_r^n(k,d)$ denotes the (k,d)th entry of matrix $\tilde{\mathbf{H}}_r^n$, and $|\cdot|_K$ denotes the mod K operator.

If the channel is time invariant, $\tilde{\mathbf{H}}_r^n$ is a circular matrix and $\mathbf{H}_r^n$ is a diagonal matrix, which means the system is ICI-free. However, for the time-varying channel, $\tilde{\mathbf{H}}_r^n$ is only pseudo-circulant and $\mathbf{H}_r^n$ becomes a full matrix, resulting in ICI. Then, (2) can be rewritten as

$$\mathbf{y}_r^n = \mathbf{H}_{r_{\text{free}}}^n\mathbf{x}^n + \mathbf{H}_{r_{\text{ICI}}}^n\mathbf{x}^n + \mathbf{n}_r^n \quad (4)$$

where $\mathbf{H}_{r_{\text{free}}}^n \triangleq \text{diag}\{[H_r^n(0,0), H_r^n(1,1), \ldots, H_r^n(K-1,K-1)]\}$ denotes the ICI-free channel matrix, and $\mathbf{H}_{r_{\text{ICI}}}^n \triangleq \mathbf{H}_r^n - \mathbf{H}_{r_{\text{free}}}^n$ is the ICI part.

C. BEM-Based Channel Model

In our previous work [18], we adopted the channel model in [7] to model the channel in the delay–Doppler domain. In this paper, however, we employ the popular BEM to model the high-mobility channel in the time domain. Assume that the channel between the transmit antenna and each receive antenna consists of L multipaths. For each channel tap l, we define $\tilde{\mathbf{h}}_r^n(l) = [h_r^n(0,l), h_r^n(1,l), \ldots, h_r^n(K-1,l)]^T \in \mathbb{C}^{K\times 1}$ as a vector that collects the time variation of the channel tap within the nth

OFDM symbol of the channel between the transmit antenna and the rth receive antenna. Denote $f_{\max}$ as the maximum Doppler shift, T as the packet duration, and $Q = 2\lceil f_{\max}T \rceil$ as the maximum number of the BEM order. Then, each $\tilde{\mathbf{h}}_r^n(l)$ can be represented as

$$\tilde{\mathbf{h}}_r^n(l) = \mathbf{B}\mathbf{c}_r^n(l) + \boldsymbol{\epsilon}_r^n(l) \tag{5}$$

where $\mathbf{B} = [\mathbf{b}_0, \ldots, \mathbf{b}_q, \ldots, \mathbf{b}_Q] \in \mathbb{C}^{K\times(Q+1)}$ collects $Q+1$ basis functions as columns; $\mathbf{b}_q$ denotes the qth basis function $(q = 0, 1, \ldots, Q)$, whose expression is related to a specific BEM model; $\mathbf{c}_r^n(l) = [c_r^n(0,l), c_r^n(1,l), \ldots, c_r^n(Q,l)]^T$ represents the BEM coefficients for the lth tap of the channel at the rth receive antenna within the nth OFDM symbol; and $\boldsymbol{\epsilon}_r^n(l) = [\epsilon_r^n(0,l), \epsilon_r^n(1,l), \ldots, \epsilon_r^n(K-1,l)]^T$ represents the BEM modeling error.

By stacking all the channel taps of the rth receive antenna within the nth OFDM symbol in one vector, i.e.,

$$\tilde{\mathbf{h}}_r^n = [h_r^n(0,0), \ldots, h_r^n(0,L-1), \ldots, h_r^n(K-1,0), \ldots h_r^n(K-1,L-1)]^T \in \mathbb{C}^{KL\times 1} \tag{6}$$

we obtain

$$\tilde{\mathbf{h}}_r^n = (\mathbf{B}\otimes\mathbf{I}_L)\mathbf{c}_r^n + \boldsymbol{\epsilon}_r^n \tag{7}$$

where $\mathbf{I}_L$ is an $L\times L$ identity matrix; $\mathbf{c}_r^n = [c_r^n(0,0), \ldots, c_r^n(0,L-1), \ldots, c_r^n(Q,0), \ldots, c_r^n(Q,L-1)]^T \in \mathbb{C}^{L(Q+1)\times 1}$ is the stacking coefficient vector; and $\boldsymbol{\epsilon}_r^n = [\epsilon_r^n(0,0), \ldots, \epsilon_r^n(0,L-1), \ldots, \epsilon_r^n(K-1,0), \ldots, \epsilon_r^n(K-1,L-1)]^T \in \mathbb{C}^{KL\times 1}$. In the following, as our focus is to discuss the performance of the channel estimator and the ICI eliminator, we ignore $\boldsymbol{\epsilon}_r^n$ for convenience. In this paper, we consider a general case where the coefficients are constant within one OFDM symbol and uncorrelated between different OFDM symbols.[2]

D. Channel Estimation and ICI Effect

From now on, with the BEM, we can describe our system in the high-mobility environment. Since we only consider the system in a single OFDM symbol in this paper, the symbol index n is omitted in the sequel for compactness. Then, substituting (7) into (2), we obtain (the detailed derivation is given in the Appendix)

$$\mathbf{y}_r = \sum_{q=0}^{Q} \mathbf{D}_q\boldsymbol{\Delta}_{r,q}\mathbf{x} + \mathbf{n}_r \tag{8}$$

where $\mathbf{D}_q = \mathbf{F}\,\mathrm{diag}\{\mathbf{b}_q\}\mathbf{F}^H$ denotes the qth BEM basis function in the frequency domain; $\boldsymbol{\Delta}_{r,q} = \mathrm{diag}\{\mathbf{F}_L\mathbf{c}_{r,q}\}$ is a diagonal matrix whose diagonal entries are the frequency responses of $\mathbf{c}_{r,q}$; $\mathbf{c}_{r,q} = [c_r(q,0), \ldots, c_r(q,L-1)]^T$ denotes the BEM coefficients of all taps of the rth receive antenna corresponding to the qth basis function; and $\mathbf{F}_L$ denotes the first L columns of $\sqrt{K}\mathbf{F}$.

Assume that $P(P<K)$ pilots are inserted in the frequency domain at the BS with the pilot pattern $\mathbf{w}$ to estimate the channel, where $\mathbf{w} = [w_1, w_2, \ldots, w_P]$. Denote $\mathbf{d}$ as the subcarrier pattern of the transmitted data. Then, the received pilot at the rth receive antenna is represented as

$$\mathbf{y}_r(\mathbf{w}) = \underbrace{\sum_{q=0}^{Q} \mathbf{D}_q(\mathbf{w},\mathbf{w})\boldsymbol{\Delta}_{r,q}(\mathbf{w},\mathbf{w})\mathbf{x}(\mathbf{w})}_{\mathbf{S}} + \underbrace{\sum_{q=0}^{Q} \mathbf{D}_q(\mathbf{w},\mathbf{d})\boldsymbol{\Delta}_{r,q}(\mathbf{d},\mathbf{d})\mathbf{x}(\mathbf{d})}_{\mathbf{G}} + \mathbf{n}_r(\mathbf{w}) \tag{9}$$

where $\mathbf{D}_q(\mathbf{w},\mathbf{w})$ and $\boldsymbol{\Delta}_{r,q}(\mathbf{w},\mathbf{w})$ represent the submatrices of $\mathbf{D}_q$ and $\boldsymbol{\Delta}_{r,q}$ with the row indexes $\mathbf{w}$ and the column indexes $\mathbf{w}$, respectively; $\mathbf{D}_q(\mathbf{w},\mathbf{d})$ represents the submatrix with the row indexes $\mathbf{w}$ and the column indexes $\mathbf{d}$; $\boldsymbol{\Delta}_{r,q}(\mathbf{d},\mathbf{d})$ represents the submatrix with the row indexes $\mathbf{d}$ and the column indexes $\mathbf{d}$; and $\mathbf{n}_r$ is the noise vector at $\mathbf{w}$. In (9), we uncouple the ICI caused by the data from the desired pilot $\mathbf{S}$ and put it in the term $\mathbf{G}$. At the receive side, it can be found that the desired $\mathbf{S}$ is distorted by $\mathbf{G}$ ($\mathbf{G} = \mathbf{0}$ for time-invariant channel, whereas $\mathbf{G} \neq \mathbf{0}$ for the time-varying channel), which can be considered additional noise and directly degrades the channel estimation accuracy. It is thus necessary to reduce the effect of ICI for a better performance.

III. Position-Based Intercarrier Intereference Elimination

Here, we show that the ICI caused by the large Doppler shift in the CE-BEM channel model can be eliminated by exploiting the train position information. This is a key finding of this paper, and based on this, we then propose a new pilot pattern design algorithm in the following.

A. Exploiting the Position Information of BEM

We first give a definition of S-sparse channels based on the BEM channel model introduced earlier.

Definition 1 (S-Sparse Channels [6]): For a BEM-based channel model given in (7), its dominant coefficients are defined as the BEM coefficients that contribute significant power, i.e., $|c_r(q,l)|^2 > \gamma$, where γ is a prefixed threshold. We say that the channel is S-sparse if the number of its dominant coefficients satisfies $S = \|\mathbf{c}_r\|_{\ell_0} \ll N_0 = L(Q+1)$, where N_0 is the total number of the BEM channel coefficients.

Then, we give the following theorem, which reflects the position information of the given system.

Theorem 1 (Position-Based S-Sparse Channels): For the considered SIMO HST system, if the high-mobility channel between the BS and each receive antenna is an S-sparse channel, which is depicted in Definition 1, then it is S-sparse at any given position.

Proof: For the considered system shown in Fig. 1, when the HST moves to a certain position at a constant speed v, the R receive antennas are at positions $\{\alpha_r\}_{r=1}^R$ and suffer from

[2]Some related works assumed that the coefficients are correlated Gaussian variables and that their variations over the OFDM blocks can be modeled by the autoregressive process. Based on this assumption, some advanced channel estimators are proposed in [21] and [22] for high-mobility systems.

different Doppler shifts $\{f_r\}_{r=1}^{R}$, respectively, where each f_r can be calculated with the known α_r supported by the GPS. Considering the HST channel has a strong line-of-sight (LOS) propagation path [23], we here assume that all the paths of each receive antenna present identical Doppler shifts. Then, according to (8), the frequency domain channel between the BS and the rth receive antenna can be represented as

$$\mathbf{H}_r = \sum_{q=0}^{Q} \mathbf{D}_q \mathbf{\Delta}_{r,q} \tag{10}$$

$$= \sum_{q=0}^{Q} \mathbf{D}_q \operatorname{diag}\{\mathbf{F}_L \mathbf{c}_{r,q}\} \tag{11}$$

where $\mathbf{D}_q$ is the known basis matrix whose expression is related to a specific BEM model, and $\mathbf{c}_{r,q}$ contains the L BEM coefficients corresponding to $\mathbf{D}_q$. Note that $q = 0, 1, \ldots, Q$ correspond to the Doppler shifts from $-f_{\max}$ to $f_{\max}$ in sequence, e.g., $q = 0$ corresponds to $-f_{\max}$ and $q = Q$ corresponds to $f_{\max}$, respectively. From (11), $\mathbf{H}_r$ is represented as the sum of the products of the qth basis matrix and its corresponding BEM coefficient vector over all Doppler shifts. Since T_r at any given position α_r suffers from a certain f_r, it can be found that $\mathbf{H}_r$ only suffers from f_r; thus, its dominant BEM coefficients only exist in $\mathbf{c}_r^*$, i.e.,

$$\mathbf{c}_r^* = \mathbf{c}_{r,q|q=q_r^*} = [c_r(q_r^*, 0), c_r(q_r^*, 1), \ldots, c_r(q_r^*, L-1)]^T \tag{12}$$

where q_r^* is called as the dominant index of the rth receive antenna corresponding to f_r. This is reasonable because, when the rth receive antenna moves to α_r, as stated previously, all its channel taps suffer from the same f_r. Thus, its dominant coefficients correspond to q_r^* and $\mathbf{c}_{r,q|q\neq q_r^*}$ can be neglected. The relationships between f_r, α_r, and q_r^* are given in the following.

Furthermore, as $\mathbf{H}_r$ is S-sparse, we have $\|\mathbf{H}_r\|_{\ell_0} = \|\mathbf{c}_r^*\|_{\ell_0} = \|\{\mathbf{c}_{r,q}\}_{q=0}^{Q}\|_{\ell_0} = S \leq L < L(Q+1)$. Since Q increases with the Doppler shift caused by fast HST speed, high mobility will introduce a large Q, and we have $S \leq L \ll L(Q+1)$. In addition, high-mobility channels are widely considered the doubly selective channels with the multipath sparsity [5]–[7], which means that there are only S paths ($S \ll L$) with large coefficients while others can be neglected. Therefore, the high-mobility channel is S-sparse at α_r, and we finally have $\|\mathbf{H}_r\|_{\ell_0} = \|\mathbf{c}_r^*\|_{\ell_0} = S \ll L \ll L(Q+1)$. ■

Accordingly, the relationship between the dominant index q_r^* and f_r is given as

$$q_r^* = \begin{cases} \lceil Tf_r \rceil + \frac{Q}{2}, & f_r \in [0, f_{\max}] \\ \lfloor Tf_r \rfloor + \frac{Q}{2}, & f_r \in [-f_{\max}, 0). \end{cases} \tag{13}$$

Denote $F = Tf_{\max} = T(v/c) \cdot f_c$. Then, the relationship between q_r^* and α_r can be represented as

$$q_r^* = \begin{cases} \left\lceil F \cdot \frac{D-\alpha_r}{\sqrt{(D-\alpha_r)^2 + D_{\min}^2}} \right\rceil + \frac{Q}{2}, & \alpha_r \in [0, D] \\ \left\lfloor F \cdot \frac{D-\alpha_r}{\sqrt{(D-\alpha_r)^2 + D_{\min}^2}} \right\rfloor + \frac{Q}{2}, & \alpha_r \in (D, 2D] \end{cases} \tag{14}$$

where $\alpha_r \in [0, D]$ denotes the rth receive antenna moving from A to B, and $\alpha_r \in (D, 2D]$ denotes moving from B to C.

From Theorem 1, we readily have the following corollary.

Corollary 1: For the considered HST system with any given train position, if the high-mobility channel between the BS and the rth ($r = 1, 2, \ldots, R$) receive antenna is S-sparse, then it can be modeled with its dominant coefficients and the dominant basis function, i.e., $\mathbf{H}_r = \mathbf{D}_r^* \mathbf{\Delta}_r^*$, where $\mathbf{\Delta}_r^* = \operatorname{diag}\{\mathbf{F}_L \mathbf{c}_r^*\}$, and $\mathbf{D}_r^* = \mathbf{D}_{q|q=q_r^*}$ is the dominant basis function of the rth receive antenna. The relationships between the dominant index q_r^*, the Doppler shift f_r, and the antenna position α_r are given as (13) and (14), respectively.

According to Corollary 1, (8) can be simplified as

$$\mathbf{y}_r = \mathbf{D}_r^* \mathbf{\Delta}_r^* \mathbf{x} + \mathbf{n}_r. \tag{15}$$

In this way, we exploit the position information of the BEM and utilize it to simplify the required channel coefficients from $L(Q+1)$ to L. Note that these analyses and conclusions are not restricted to any specific BEM.

B. Position-Based ICI Elimination

Here, we consider the CE-BEM [25] due to its independence of the channel statistics, and it is strictly banded in the frequency domain. In particular, for the CE-BEM, the qth basis function $\mathbf{b}_q$ can be represented as

$$\mathbf{b}_q = \left[1, \ \ldots, \ e^{j\frac{2\pi}{K}k(q-\frac{Q}{2})}, \ \ldots, \ e^{j\frac{2\pi}{K}(K-1)(q-\frac{Q}{2})}\right]^T. \tag{16}$$

Then, $\mathbf{D}_q$ can be written as

$$\mathbf{D}_q = \mathbf{F} \operatorname{diag}\{\mathbf{b}_q\} \mathbf{F}^H = \mathbf{I}_K^{\langle q-\frac{Q}{2}\rangle} \mathbf{F}\mathbf{F}^H \tag{17}$$

$$= \mathbf{I}_K^{\langle q-\frac{Q}{2}\rangle} \tag{18}$$

where $\mathbf{I}_K^{\langle q-(Q/2)\rangle}$ denotes a matrix obtained from a $K \times K$ identity matrix $\mathbf{I}_K$ with a permutation $q - Q/2$. Then, we have

$$\mathbf{H}_r = \sum_{q=0}^{Q} \mathbf{I}_K^{\langle q-\frac{Q}{2}\rangle} \mathbf{\Delta}_{r,q}. \tag{19}$$

By detecting the matrix structure, we find that $\mathbf{H}_r$ is strictly banded with the bandwidth $Q+1$, which means that the Q neighboring subcarriers give rise to interference, i.e., the desired signal suffers from the ICI from the Q neighboring subcarriers.

Let us consider Corollary 1; then, the dominant basis $\mathbf{D}_r^*$ for the CE-BEM can be rewritten as

$$\mathbf{D}_r^* = \mathbf{I}_K^{\langle q_r^*-\frac{Q}{2}\rangle}. \tag{20}$$

Similarly, we have

$$\mathbf{H}_r = \mathbf{I}_K^{\langle q_r^*-\frac{Q}{2}\rangle} \mathbf{\Delta}_r^* \tag{21}$$

where $\mathbf{H}_r$ becomes a diagonal matrix with a permutation, and its nonzero entries are corresponding to the dominant coefficients. From (21), we find that, with Corollary 1, the desired signal is free of ICI but with a permutation of the received subcarrier. This is reasonable because the dominant coefficients in $\mathbf{c}_r^*$, corresponding to f_r, describe the channel alone, whereas the nondominant ones can be ignored. Therefore, by utilizing the position information, we can get the ICI-free pilots at the receive side and reduce the needed channel coefficients from KL to L.

Remark 1: With Corollary 1, the conclusion that $\mathbf{H}_r$ is a permutated diagonal matrix only holds for the CE-BEM since $\mathbf{D}_q$ itself is a permutated identity matrix for the CE-BEM. For other BEMs, e.g., the GCE-BEM [26], the P-BEM [27], and the DPS-BEM [28], $\mathbf{D}_q$ is approximately banded. However, it can be expected that the proposed method can also highly reduce the ICI for other BEMs for only considering the dominant coefficients.

Assume $\mathbf{w}$ is received at the rth receive antenna with the pilot pattern $\mathbf{v}_r = [v_{r,1}, v_{r,2}, \ldots, v_{r,P}]$. Then, with Corollary 1, (9) can be rewritten as

$$\begin{aligned}\mathbf{y}_r(\mathbf{v}_r) &= \mathbf{D}_r^*(\mathbf{v}_r, \mathbf{w})\boldsymbol{\Delta}_r^*(\mathbf{w}, \mathbf{w})\mathbf{x}(\mathbf{w}) \\ &\quad + \underbrace{\mathbf{D}_r^*(\mathbf{v}_r, \mathbf{d})\boldsymbol{\Delta}_r^*(\mathbf{d}, \mathbf{d})\mathbf{x}(\mathbf{d})}_{\mathbf{G}^*} + \mathbf{n}_r(\mathbf{v}_r) \qquad (22) \\ &= \mathbf{D}_r^*(\mathbf{v}_r, \mathbf{w})\boldsymbol{\Delta}_r^*(\mathbf{w}, \mathbf{w})\mathbf{x}(\mathbf{w}) + \mathbf{n}_r(\mathbf{v}_r) \qquad (23)\end{aligned}$$

where $\mathbf{D}_r^*(\mathbf{v}_r, \mathbf{w})$ represents its submatrix with the row indexes $\mathbf{v}_r$ and the column indexes $\mathbf{w}$; $\boldsymbol{\Delta}_r^*(\mathbf{w}, \mathbf{w})$ represents its submatrix with the row indexes $\mathbf{w}$ and the column indexes $\mathbf{w}$; $\mathbf{D}_r^*(\mathbf{v}_r, \mathbf{d})$ represents its submatrix with the row indexes $\mathbf{v}_r$ and the column indexes $\mathbf{d}$; and $\boldsymbol{\Delta}_r^*(\mathbf{d}, \mathbf{d})$ represents its submatrix with the row indexes $\mathbf{d}$ and the column indexes $\mathbf{d}$. In (23), the term $\mathbf{G}^*$ denotes the ICI caused by the data, and we have $\mathbf{G}^* = \mathbf{0}$ since its corresponding entries of the dominant basis are zero, i.e., $\mathbf{D}_r^*(\mathbf{v}_r, \mathbf{d}) = \mathbf{0}$. Thus, it is easy to find the received pilots are free of the ICI but with a permutation of the received subcarriers. The relationship between $\mathbf{v}_r$ and $\mathbf{w}$ is given as

$$v_{r,p} = \left| w_p + \left(q_r^* - \frac{Q}{2} \right) \right|_K, \quad w_p \in \mathbf{w}; \quad v_{r,p} \in \mathbf{v}_r \qquad (24)$$

where $p = 1, 2, \ldots, P$; and $|\cdot|_K$ denotes the mod K operator.

For better clarification, we plot the structure of $\mathbf{H}_r$ in Fig. 2. The columns of $\mathbf{H}_r$ are related to the subcarriers of the transmitted pilots and data, which operate on $\mathbf{D}_q$ through $\boldsymbol{\Delta}_{r,q}$. The rows of $\mathbf{H}_r$ are related to the subcarriers of the received signals at the rth receive antenna. For the CE-BEM, $\mathbf{H}_r$ is strictly banded with the bandwidth $Q + 1$, which is shown as the gray parts. In Fig. 2, it can be observed that a received signal $Y_r(w_p)$ suffers from the ICI from the Q neighboring subcarriers of its desired signal $X(w_p)$, which is shown as the blue dash dot line. Then, with Corollary 1, $\mathbf{H}_r$ turns to the green solid line, and the gray parts can be neglected, which is because the dominant coefficients alone describe the channel with the Doppler shift f_r. It is easy to find that the desired signal $X(w_p)$ is free of the ICI but received at $Y(v_{r,p})$ with a permutation of the received subcarrier, which is shown as the red dashed lines. Therefore, with the proposed method, the ICI among the received pilots at each receive antenna is eliminated.

IV. Low-Coherence Compressed Channel Estimation

Here, based on the proposed ICI elimination method, we design the pilot pattern to minimize the system average coherence and hence can improve the CS-based channel estimation performance. First, we briefly review some fundamentals of CS. Then, we formulate the problem and propose a new pilot pattern design algorithm to solve it. Finally, we discuss the complexity and practical applicability of our scheme.

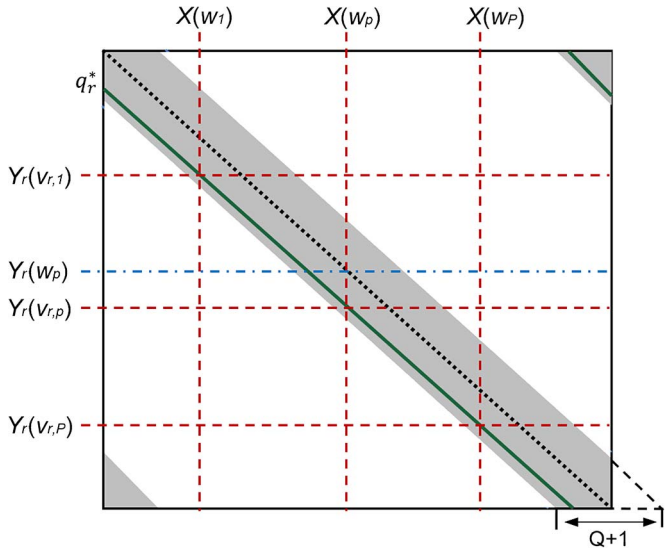

Fig. 2. Structure of $\mathbf{H}_r$. The gray parts denote the nonzero entries of $\mathbf{H}_r$, and the white parts denote the zero entries. The green solid line denotes the entries corresponding to the dominant basis function $\mathbf{D}_r^*$ with the dominant index q_r^*. The black dot line denotes the diagonal entries of $\mathbf{H}_r$.

A. CS Fundamentals

CS is an innovative technique to reconstruct sparse signals accurately from a limited number of measurements. Considering an unknown signal $\hat{\mathbf{x}} \in \mathbb{C}^M$, suppose that we have $\hat{\mathbf{x}} = \boldsymbol{\Phi}\mathbf{a}$, where $\boldsymbol{\Phi} \in \mathbb{C}^{M \times U}$ denotes a known dictionary matrix, and $\mathbf{a} \in \mathbb{C}^U$ denotes a S-sparse vector, i.e., $\|\mathbf{a}\|_{\ell_0} = S \ll U$. Then, CS considers the following problem:

$$\hat{\mathbf{y}} = \boldsymbol{\Psi}\hat{\mathbf{x}} + \boldsymbol{\eta} = \boldsymbol{\Psi}\boldsymbol{\Phi}\mathbf{a} + \boldsymbol{\eta} \qquad (25)$$

where $\boldsymbol{\Psi} \in \mathbb{C}^{V \times M}$ presents a known measurement matrix, $\hat{\mathbf{y}} \in \mathbb{C}^V$ presents the observed vector, and $\boldsymbol{\eta} \in \mathbb{C}^V$ is the noise vector. The objective of CS is to reconstruct $\mathbf{a}$ accurately based on the knowledge of $\hat{\mathbf{y}}$, $\boldsymbol{\Psi}$, and $\boldsymbol{\Phi}$. It has been proved in [13] that if $\boldsymbol{\Psi}\boldsymbol{\Phi}$ satisfies the restricted isometry property [29], then $\mathbf{a}$ can be reconstructed accurately with CS reconstruction methods, such as the basis pursuit (BP) [30] and the orthogonal matching pursuit (OMP) [31]. In addition, a fundamental research [14] indicates that the average coherence reflects the actual CS behavior rather than the mutual coherence [12] for considering the average performance. The definition of the average coherence is given as follows.

Definition 2 (Average Coherence [14]): For a matrix $\mathbf{M}$ with the ith column as $\mathbf{g}_i$, its average coherence is defined as the average of all absolute inner products between any two normalized columns in $\mathbf{M}$ that are beyond a threshold δ, where $0 < \delta < 1$. Put formally

$$\mu_\delta\{\mathbf{M}\} = \frac{\sum\limits_{i \neq j} (|g_{ij}| \geq \delta) \cdot |g_{ij}|}{\sum\limits_{i \neq j} (|g_{ij}| \geq \delta)} \qquad (26)$$

where $g_{ij}=\tilde{\mathbf{g}}_i^H\tilde{\mathbf{g}}_j$, $\tilde{\mathbf{g}}_i=\mathbf{g}_i/\|\mathbf{g}_i\|_{\ell_2}$, and the operator is defined as

$$(x\geq y)=\begin{cases}1, & x\geq y\\ 0, & x<y.\end{cases} \tag{27}$$

It has been established in [14] that a smaller $\mu_\delta\{\mathbf{\Psi\Phi}\}$ will lead to a more accurate recovery of $\mathbf{a}$. From this point of view, it can be expected that, if $\mathbf{\Psi}$ is designed with a fixed $\mathbf{\Phi}$ such that $\mu_\delta\{\mathbf{\Psi\Phi}\}$ is as small as possible, then CS can get better recovery performance.

B. Problem Formulation

To utilize the sparsity of the high-mobility channel according to Theorem 1, we rewrite the received pilots at the rth antenna as a function of channel coefficients. In this paper, we assume that each receive antenna estimates its channel individually and then sends the estimated channel to the RS for operation. Then, (23) can be rewritten as

$$\mathbf{y}_r(\mathbf{v}_r)=\mathbf{D}_r^*(\mathbf{v}_r,\mathbf{w})\mathbf{S}(\mathbf{w},:)\mathbf{c}_r^*+\mathbf{n}_r(\mathbf{v}_r) \tag{28}$$

where $\mathbf{S}(\mathbf{w},:)=\mathrm{diag}\{\mathbf{x}(\mathbf{w})\}\mathbf{F}_L(\mathbf{w},:)$. In this way, the task of estimating the high-mobility channel $\mathbf{H}_r$ in the frequency domain is converted to estimating the sparse coefficient vector $\mathbf{c}_r^*$.

As mentioned earlier, we have known that a lower μ_δ leads to a better CS performance. Therefore, we propose to design the pilot pattern $\mathbf{w}$ to minimize the average coherence in our system. In this paper, we only design the pilot pattern and assume the pilot symbols are the same. Therefore, the global pilot pattern design problem can be formulated as

$$\mathbf{w}^*=\arg\min_{\mathbf{w}}\max_r\mu_\delta\left\{\mathbf{D}_r^*(\mathbf{v}_r,\mathbf{w})\mathbf{S}(\mathbf{w},:)\right\} \tag{29}$$

where $\mathbf{w}^*$ denotes the optimal pilot pattern; and $r=1,2,\ldots,R$. Note that, for a given $\mathbf{w}$, its corresponding $\mathbf{v}_r$ at the rth receive antenna can be obtained by (24). Thus, $\mathbf{w}$ is the only variable in this problem.

Taking the expression of $\mathbf{D}_r^*$ into consideration, the objective function can be represented as

$$\begin{aligned}&\mu_\delta\left\{\mathbf{D}_r^*(\mathbf{v}_r,\mathbf{w})\mathbf{S}(\mathbf{w},:)\right\}\\ &\quad=\mu_\delta\left\{\mathbf{I}_K^{\langle q_r^*-\frac{Q}{2}\rangle}(\mathbf{v}_r,\mathbf{w})\mathrm{diag}\left\{\mathbf{x}(\mathbf{w})\right\}\mathbf{F}_L(\mathbf{w},:)\right\} &(30)\\ &\quad=\mu_\delta\left\{\mathrm{diag}\left\{\mathbf{x}(\mathbf{w})\right\}\mathbf{F}_L(\mathbf{w},:)\right\} &(31)\end{aligned}$$

where $\mathbf{F}_L(\mathbf{w},:)$ denotes the submatrix of $\mathbf{F}_L$ with the row indexes $\mathbf{w}$ and all columns. Here, we have $\mathbf{I}_K^{\langle q_r^*-(Q/2)\rangle}(\mathbf{v}_r,\mathbf{w})=\mathbf{I}_P$ for $r=1,2,\ldots,R$, and $\mathbf{I}_P$ denotes a $P\times P$ identity matrix. This is because $\mathbf{v}_r$ and $\mathbf{w}$ are designed by (24) to select the nonzero entries of $\mathbf{D}_r^*$.

Suppose that each pilot symbol has the same constant amplitude, i.e.,

$$|X(w_p)|^2=A\quad\forall\, w_p\in\mathbf{w}. \tag{32}$$

According to Definition 2, it is not difficult to prove that the average coherence is independent of the constant amplitude. Thus, the objective function can be further written as

$$\begin{aligned}\mu_\delta\left\{\mathbf{D}_r^*(\mathbf{v}_r,\mathbf{w})\mathbf{S}(\mathbf{w},:)\right\}&=\mu_\delta\left\{A\mathbf{F}_L(\mathbf{w},:)\right\} &(33)\\ &=\mu_\delta\left\{\mathbf{F}_L(\mathbf{w},:)\right\}. &(34)\end{aligned}$$

In this way, problem (29) is simplified to the following optimization problem:

$$\mathbf{w}^*=\arg\min_{\mathbf{w}}\mu_\delta\left\{\mathbf{F}_L(\mathbf{w},:)\right\}. \tag{35}$$

From (35), we find that the optimal pilot pattern $\mathbf{w}^*$ is independent of the train speed v, the Doppler shift f_r, the antenna number R, or the antenna position α_r. This means that $\mathbf{w}^*$ is global optimal, regardless of the receive antenna number, the antenna position, the Doppler shift, or the train speed. Thus, for the given system, we can predesign $\mathbf{w}^*$ and then sends it to each receive antenna to estimate the channel during the whole system runs. Note that the problem (35) is different from the problem in our previous work [18], where the optimal pilot was related to the Doppler shift according to the instant train position.

C. Low-Coherence Pilot Pattern Design

The similar pilot design problems for SISO-OFDM systems have been studied in [19] and our previous work [18]. However, these methods cannot be directly applied to (35). The problem in [19] includes the guard pilots and needs to follow some constraints to eliminate the ICI. In addition, the optimal pilot in [18] is related to the instant train position. Here, following the spirit of [18], we propose a low-complexity suboptimal pilot pattern design algorithm to solve this problem. The details are presented in Algorithm 1.

Algorithm 1 Low Coherence Pilot Pattern Design

Input: Initial pilot pattern $\mathbf{w}$.
Output: Optimal pilot pattern $\mathbf{w}^*=\hat{\mathbf{w}}^{(MP)}$.
1: **Initialization**: Set Iter$=M\times P$, set $\mathbf{\Gamma}=\mathbf{0}$ and $\Gamma[0,0]=1$, set $\kappa=0$ and $\iota=0$.
2: **for** $n=0,1,\ldots,M-1$ **do**
3: **for** $k=0,1,\ldots,P-1$ **do**
4: $m=n\times P+k$;
a) Generate new pilot pattern:
5: generate $\tilde{\mathbf{w}}^{(m)}$ with operator $\mathbf{w}^{(m)}\Rightarrow\tilde{\mathbf{w}}^{(m)}$;
6: **If** $\mu_\delta\{\mathbf{F}_L(\tilde{\mathbf{w}}^{(m)},:)\}<\mu_\delta\{\mathbf{F}_L(\mathbf{w}^{(m)},:)\}$ **then**
7: $\mathbf{w}^{(m+1)}=\tilde{\mathbf{w}}^{(m)}$; $\kappa=m+1$;
8: **else**
9: $\mathbf{w}^{(m+1)}=\mathbf{w}^{(m)}$;
10: **end if**
b) Update state occupation probability and pilot pattern:
11: $\mathbf{\Gamma}[m+1]=\mathbf{\Gamma}[m]+\eta[m](\mathbf{U}[m+1]-\mathbf{\Gamma}[m])$, with $\eta[m]=(1/(m+1))$;
12: **if** $\Gamma[m+1,\kappa]>\Gamma[m+1,\iota]$
13: $\hat{\mathbf{w}}^{(m+1)}=\mathbf{w}^{(m+1)}$; $\iota\Leftarrow\kappa$;
14: **else**
15: $\hat{\mathbf{w}}^{(m+1)}=\hat{\mathbf{w}}^{(m)}$;
16: **end if**
17: **end for** (k)
18: **end for** (n)

In Algorithm 1, $\mathbf{w}^{(m)}$, $\tilde{\mathbf{w}}^{(m)}$, and $\hat{\mathbf{w}}^{(m)}$ are defined as different pilot pattern sets at the mth iteration. M is the number of pilot pattern sets, and Iter $= M \times P$ denotes the total iteration times. The probability vector $\mathbf{\Gamma}[m] = [\Gamma[m,1], \Gamma[m,2], \ldots, \Gamma[m,MP]]^T$ represents the state occupation probabilities with entries $\Gamma[m,\kappa] \in [0,1]$, and $\sum_\kappa \Gamma[m,\kappa] = 1$. $\mathbf{U}[m] \in \mathbb{R}^{MP\times 1}$ is defined as a zero vector, except for its mth entry, which is 1. In Step a, $\tilde{\mathbf{w}}^{(m)}$ is obtained with the operator $\mathbf{w}^{(m)} \Rightarrow \tilde{\mathbf{w}}^{(m)}$, which is defined as follows: At the mth iteration, the kth pilot subcarrier of $\mathbf{w}^{(m)}$ is replaced with a random subcarrier, which is not included in $\mathbf{w}^{(m)}$. Then, we compare $\tilde{\mathbf{w}}^{(m)}$ with $\mathbf{w}^{(m)}$ and select the one with a smaller system coherence to move a step. In Step b, $\mathbf{\Gamma}[m+1]$ is updated based on the previous $\mathbf{\Gamma}[m]$ with the decreasing step size $\eta[m] = 1/(m+1)$. The current optimal pattern is updated by selecting the pilot pattern with the largest occupation probability. Finally, the optimal pilot pattern is obtained as $\mathbf{w}^* = \hat{\mathbf{w}}^{(MP)}$. According to [18], this process can quickly converge to the optimal solution.

Remark 2: In contrast to the work in [19], Algorithm 1 does not need any guard pilot to eliminate the ICI, which highly improves the spectral efficiency. This is because the received pilots are ICI free at each receive antenna with the proposed ICI elimination method. In particular, the total needed pilot number in [19] is $(2Q+1)P$ (P effective pilots and $2QP$ guard pilots), whereas our method only needs P pilots.

D. Complexity Analysis

Here, we briefly discuss the complexity of our proposed scheme. The complexity is mainly determined by the number of the needed complex multiplications. The complexity of the proposed scheme mainly consists of two parts: the low coherence pilot pattern design (see Algorithm 1) and the position-based ICI elimination.

- For Algorithm 1, $MP^2(L(L-1)+M)$ complex multiplications are required in total. In a practical system, as the constant parameters M, L, and P are much smaller than K, the complexity of Algorithm 1 is much lower than $\mathcal{O}(K^2)$. Furthermore, since the needed system parameters can be estimated in advance, Algorithm 1 is an offline process; thus, its complexity can be omitted in practice.
- For our ICI elimination method, with known the optimal pilot pattern predesigned by Algorithm 1, the rth antenna obtains its receive pilot pattern by (24) at any given position. This process only needs a permutation of the subcarriers, where the needed q_r^* can be directly calculated from the HST's current speed and position information supported by the GPS. Thus, the proposed ICI elimination method introduces very low complexity in practical systems.

In addition, we also compare the system complexity of the proposed scheme and the scheme in our previous work [18] in SIMO systems. Note that the scheme in [18] cannot directly extend to the SIMO system. For SIMO systems, since the length of the HST cannot be ignored comparing with the cell range in practice, the receive antennas may suffer from different Doppler shifts and correspond to different optimal pilots. To solve this problem, based on the scheme in [18], one may divide the total P pilots into R subsets, and each subset sends the corresponding optimal pilot for each receive antenna to minimize the system coherence. In the presence of a large number of the receive antennas (i.e., large R), this method will introduce high system complexity for selecting different optimal pilots. In addition, since the effective pilot number for each receive antenna is P/R, a large R will also highly reduce the spectral efficiency for needing more total pilots to get satisfactory estimation performance. However, for the proposed method in this paper, since $\mathbf{w}^*$ is independent of the receive antenna position and receive antenna number, with increasing R, each receive antenna can still have P effective pilots.

E. Practical Applicability

Now, we briefly discuss the applicability of the proposed scheme in a practical HST system. The entire process of our proposed scheme is summarized as follows.

1) For a given HST system, as the system parameters can be collected in advance, the optimal pilot pattern $\mathbf{w}^*$ is predesigned by Algorithm 1 and then prestored at both the BS and the HST. Since $\mathbf{w}^*$ is independent of the Doppler shift or the train position, the BS transmits $\mathbf{w}^*$ to estimate the channels during the whole process. In contrast, in our previous work [18], the BS was required to select different optimal pilot for each receive antenna from a predesigned codebook according to the instant train position, which introduces high system complexity.
2) Then, the antennas on the HST receive the signals and get the ICI-free pilots with the proposed ICI elimination method, which is given as (24). In addition, with the instant train position and speed information supported by the GPS, q_r^* of each receive antenna can be easily calculated with the given (13) and (14).
3) After that, each receive antenna uses the ICI-free pilots to estimate the channel coefficients with the conventional CS estimators.

In this way, the proposed scheme can be well used in current HST systems without adding too much complexity. Note that, as $\mathbf{w}^*$ is also independent of the train speed, the performance of the proposed scheme is robust to the high mobility. This is interesting because that the channel estimation performances are always highly influenced by the high system mobility [18], [20]. In the following, we will give some simulation results to demonstrate the effectiveness of the proposed algorithm.

V. Simulation Results

Here, we present the performance of the proposed scheme by two typical compressed channel estimators: BP [30] and OMP [31]. The MSE at each individual receive antenna and the bit error rate (BER) at the RS are illustrated versus the SNR at different HST positions. We assume that the $R = 2$ receive antennas are equipped, one at the front and the other at the end of the HST, respectively, i.e., the distance between the two receive antennas is equal to the HST length. The HST system parameters are given in Table I. We consider a 512-subcarrier OFDM system with 40 pilot subcarriers, and the carrier frequency

TABLE I
HST COMMUNICATION SYSTEM PARAMETERS

Parameters	Variables	Values
BS cover range	R_{BS}	1000 m
HST length	L_{hst}	200 m
Max distance of BS to railway	D_{max}	1000 m
Min distance of BS to railway	D_{min}	40 m
Carrier frequency	f_c	2.35 GHz
Train speed	v	500 km/h

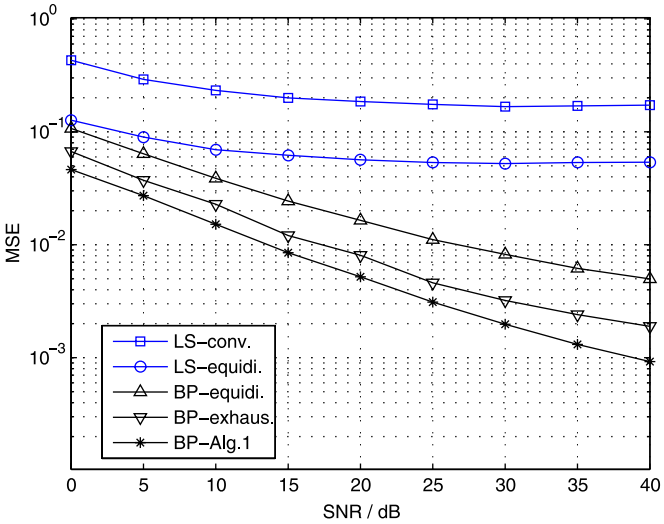

Fig. 3. MSE performances of LS and the BP estimators with different pilots at the position A.

is $f_c = 2.35$ GHz. The bandwidth is set to be 5 MHz, the packet duration is $T = 1.2$ ms, and the modulation is 4-ary quadrature amplitude modulation (4-QAM). We consider the CE-BEM channel model; each channel has $L = 64$ taps, and only five taps are dominant ones with random positions. The speed of the HST is 500 km/h, which means that the maximum Doppler shift is $f_{\max} = 1.087$ kHz. As a benchmark, the iterative ICI mitigation method in [20] is simulated to compare with our proposed position-based ICI elimination method.

A. MSE Performances

Fig. 3 gives the comparison of the MSE performances of different estimators with different pilot patterns at the position A, where the Doppler shift at the receive antenna is 1.087 kHz. In this figure, we compare three pilot pattern design methods. The equidistant method ("equidi.") is the equidistant pilot pattern in [4], which is claimed in [4] as the optimal pilot pattern to doubly selective channels. The exhaustive method ("exhaust.") is the method in [15] with 200 iterations, which does an exhaustive search from a designed pilot pattern set. The iteration time of Algorithm 1 is set to be Iter $= 200$, where it is shown in [18] that Iter $= 200$ is good enough for a practical system. The "LS-equidi." method, the "BP-equidi." method, the "BP-exhaus." method, and the "BP-Alg.1" method are equipped with the proposed ICI elimination method. In addition, the conventional LS method with the equidistant pilot pattern ("LS-conv.") is equipped with the ICI mitigation method in [20] with two

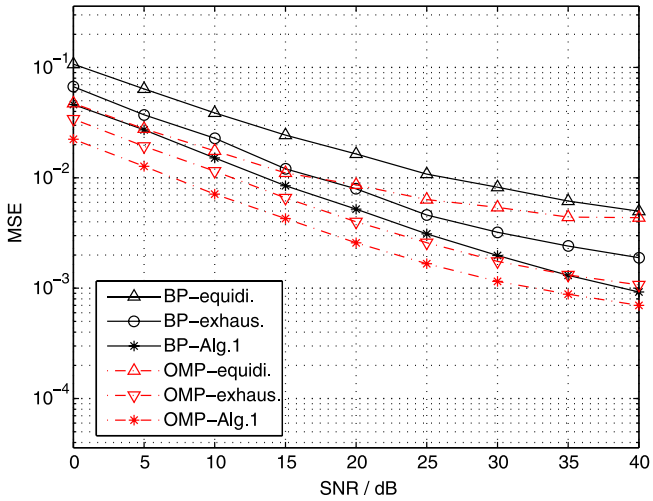

Fig. 4. MSE performances of BP and the OMP estimators with different pilots at the position C.

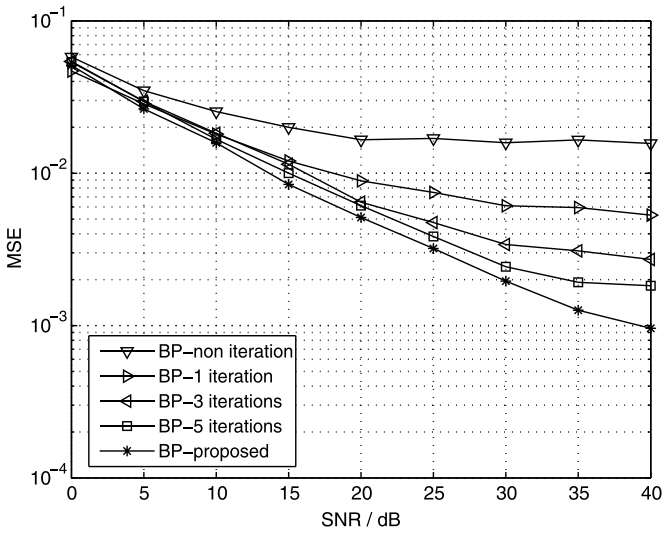

Fig. 5. MSE performances of BP estimators with different ICI elimination methods, $\alpha_r = 900$ m, and $f_r = 1.009$ KHz.

iteration times. It can be observed that the BP estimators significantly improve the performances than the LS methods by utilizing the sparsity of the high-mobility channels. Furthermore, it is found that the estimators with the proposed ICI elimination method get better performances than the one with the conventional method, which means that the proposed method effectively eliminates the ICI. As expected, comparing with other pilot patterns, Algorithm 1 improves the MSE performance for effectively reducing the system average coherence.

Fig. 4 shows the comparison of the MSE performances of BP and OMP estimators versus SNR with different pilot patterns at the position C, where the Doppler shift at the receive antenna is -1.087 kHz. All of BP and OMP estimators are considered with the proposed ICI elimination method. As can be seen, with Algorithm 1, both BP and OMP get better performances compared with other pilot patterns. It can be seen that the proposed algorithm is effective to both BP and OMP estimators.

Fig. 5 presents the MSE performances of BP estimators versus SNR with the proposed ICI elimination method and

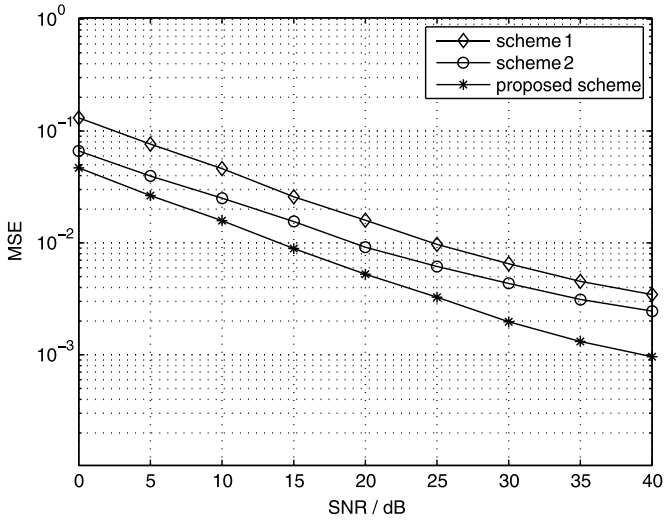

Fig. 6. Comparison of the MES performances of different schemes.

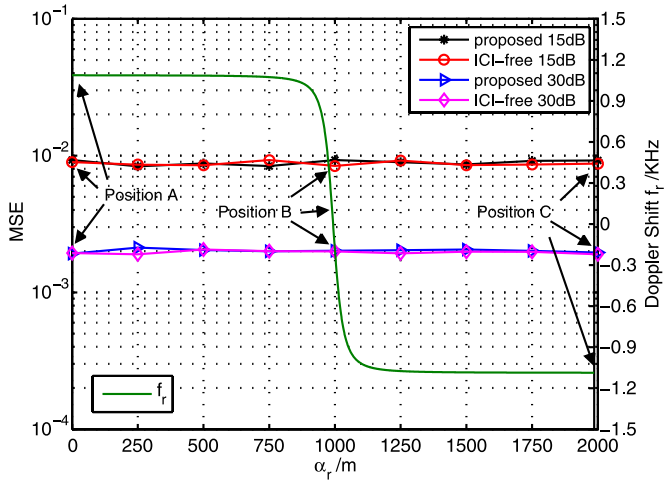

Fig. 7. MSE performances of BP estimators with Algorithm 1 and the Doppler shift versus the antenna position α_r.

the conventional ICI mitigation method, where the Doppler shift at the receive antenna is $f_r = 1.009$ KHz according to $\alpha_r = 900$ m. The ICI mitigation is considered with the iteration time as 0, 1, 3, and 5 to show the performance tendency. All of these estimators are equipped with the pilot pattern designed by Algorithm 1 (Iter $= 200$). It can be observed that, under a large Doppler shift, the estimation performance without considering ICI ("noniteration") is significantly degraded due to the pilots are distorted by the induced ICI, which greatly affects system performance. Thus, it is necessary to operate the ICI elimination in high-mobility environment. In addition, with increasing iterations, the BP with the ICI mitigation method converges to the one with the proposed ICI elimination method, which gets the ICI-free pilots as aforementioned analysis. We also notice that the ICI mitigation gain is limited with increasing iteration times due to the error propagation.

Fig. 6 compares the MSE performances versus SNR of the proposed scheme, the scheme 1 in [18], and the scheme 2 in [19], where the Doppler shift at the receive antenna is $f_r = 1.087$ KHz. The proposed scheme and the scheme in [18] are both considered with 40 pilots and equipped with the proposed ICI elimination method. However, since the optimal pilot in [18] is related to the instant antenna position, we divide the 40 pilots into two sets to send the optimal pilots for each antenna (20 effective pilots for each one). In addition, the scheme in [19] is considered with the guard pilots to get the ICI-free structure, and its total pilot number is 243. Note that it needs 216 guard pilots to eliminate the ICI; thus, its effective pilot number is 27. In this figure, it can be observed that the proposed scheme gets better performance with the same pilot number as [18]. It is mainly because the optimal pilot for the proposed scheme is independent of the instant antenna position, i.e., the R receive antennas correspond to the same optimal pilot; thus, each receive antenna has 40 effective pilots. Furthermore, we notice that the proposed scheme is better than the scheme in [19] with less pilot number. This is because the proposed ICI elimination method only needs a permutation of the receive subcarriers without needing any guard pilot, which greatly improves spectral efficiency.

Fig. 7 presents the MSE performances of BP estimators versus the receive antenna position at SNR $= 15$ dB and SNR $=$ 30 dB. As a reference, we also plot the Doppler shift f_r at the rth receive antenna versus its position $\alpha_r \in [0, 2000]$m (from A to C). We can find that f_r changes from $f_{\max}$ to $-f_{\max}$ with the HST moves, and it changes rapidly near the position B. In this figure, the resulting curves correspond to the performances when the proposed ICI elimination method is performed and when the estimation considers that pilots are free of ICI ("ICI-free") at SNR $= 15$ and 30 dB, respectively. When the pilots are free of ICI, it means that the transmitted OFDM symbol is set as zero at the data subcarriers. All estimators are considered with the pilot pattern designed by Algorithm 1 (Iter $= 200$). From the curves, it can be observed that the proposed method and the ICI-free method are almost superimposed, which means that the proposed method can effectively obtain the ICI-free pilots. In addition, we also notice that, although the HST suffers from large Doppler shift at most of the positions and f_r changes rapidly near B, the MSE performances of the proposed method are stable. This is because the optimal pilot pattern and the proposed ICI elimination method are both independent of the position information and the system mobility. Thus, the proposed scheme is robust with respect to mobility and the variation of Doppler shift. Furthermore, since the conventional scheme with nonideal ICI compensation is always significantly influenced by mobility (see [18, Fig. 9]), it is necessary to find a new channel estimation method with robust ICI elimination.

B. BER Performances

Fig. 8 shows the BER performances versus SNR of the 1×2 SIMO-OFDM system in the given high-mobility environment at the position A, where the Doppler shifts at the receive antennas are both 1.087 kHz. In this figure, we compare the LS, the BP, and the OMP estimators with the pilot patterns designed by the equidistant method, the exhaustive method, and Algorithm 1 (Iter $= 200$). The conventional LS method ("LS-conv.") is considered with the one-tap equalization, and other methods are considered with the zero-forcing (ZF) equalizer. As a reference, we also plot the performance with the perfect knowledge of

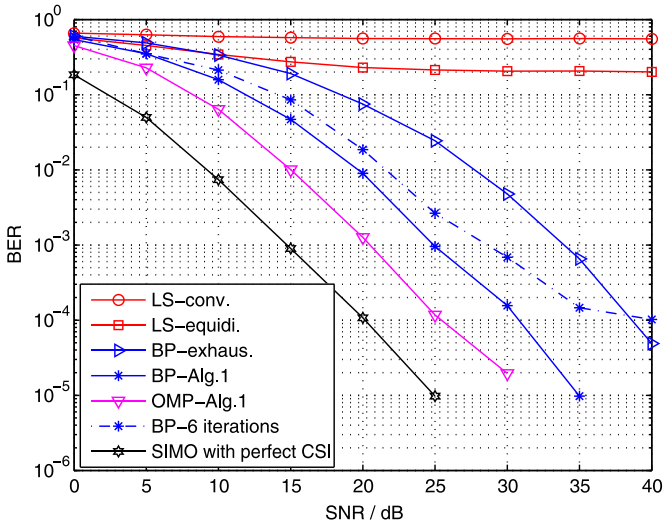

Fig. 8. BER performances of the 1×2 SIMO-OFDM system.

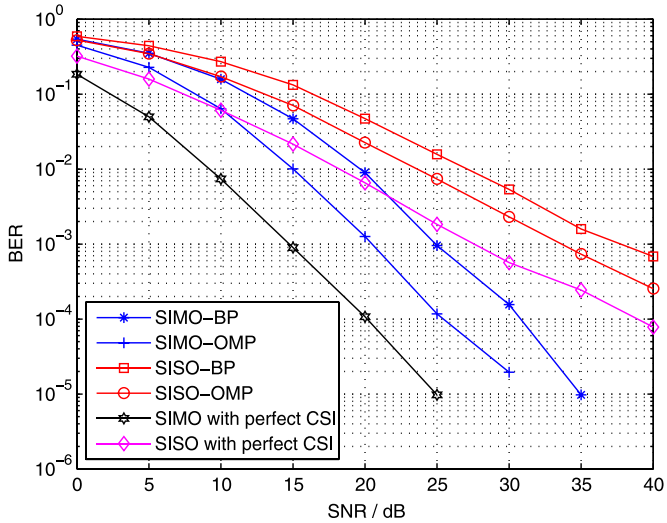

Fig. 9. BER performances of SIMO and SISO systems.

channel state information (CSI), which means that the CSI is available at the RS and employed with the ZF equalizer. In addition, the BP estimator with Algorithm 1, and the ICI mitigation method of six iteration times is also considered. As shown, BP and OMP with Algorithm 1 are closer to the perfect knowledge of CSI. It is also shown that "BP-Alg.1" with the proposed ICI elimination method outperforms the one with the conventional ICI mitigation method for effectively eliminating the ICI. In addition, it can be observed that the pilot pattern designed by Algorithm 1 significantly improves the performances for effectively reducing the system coherence.

Fig. 9 compares the BER performances between the 1×2 SIMO-OFDM system and the SISO-OFDM system in the given high-mobility environment at position A. Both of the SIMO and SISO systems are considered with 40 pilots. All estimators are equipped with the pilot pattern designed by Algorithm 1 and the proposed ICI elimination method. As a reference, we plot the performances with the perfect knowledge of CSI for both the SIMO and SISO systems. It can be observed that the SIMO system significantly improves the BER performances due to the spatial diversity introduced by multiple antennas.

VI. Conclusion

In this paper, for the considered SIMO-OFDM HST communication system, we exploit the train position information and utilize it to mitigate the ICI caused by the high mobility. In particular, for the CE-BEM, we propose a new low-complexity ICI elimination method to get the ICI-free pilots at each receive antenna. Furthermore, we design the pilot pattern to minimize the system coherence and hence can improve the CS-based channel estimation performance. Simulation results demonstrate that the proposed scheme achieves better performances than the existing methods in the high-mobility environment. In addition, it is also shown that the proposed scheme is robust to high mobility.

Appendix
Derivation of (8)

For the sake of compactness, the symbol index n is omitted here. Since we assume that there are L multipaths, we have $h_r(k,l)=0(l > L-1)$, and $\tilde{\mathbf{H}}_r$ in (3) can be expressed as (36), shown at the bottom of the page. According to (5), we have

$$h_r(k,l) = \sum_{q=0}^{Q} b_q(k) c_r(q,l) \tag{37}$$

where $b_q(k)$ denotes the kth entry of the vector $\mathbf{b}_q$, and $\mathbf{b}_q \triangleq [b_q(0), \ldots, b_q(K-1)]^T$.

Then, taking (37) into (36) and after some algebra, $\tilde{\mathbf{H}}_r$ can be represented as a matrix form:

$$\tilde{\mathbf{H}}_r = \sum_{q=0}^{Q} \tilde{\mathbf{D}}_q \mathbf{G}_{r,q} \tag{38}$$

$$\tilde{\mathbf{H}}_r = \begin{bmatrix} h_r(0,0) & 0 & \cdots & 0 & h_r(0,L-1) & \cdots & h_r(0,1) \\ h_r(1,1) & h_r(1,0) & 0 & \cdots & 0 & \cdots & h_r(1,2) \\ \vdots & \ddots & \ddots & \ddots & \ddots & \ddots & \vdots \\ h_r(L-1,L-1) & \ddots & \ddots & \ddots & \ddots & \ddots & 0 \\ 0 & \ddots & \ddots & \ddots & \ddots & \ddots & 0 \\ 0 & \cdots & \cdots & h_r(K-1,L-1) & \cdots & \cdots & h_r(K-1,0) \end{bmatrix} \tag{36}$$

where $\tilde{\mathbf{D}}_q = \mathrm{diag}\{\mathbf{b}_q\}$; $\mathbf{G}_{r,q}$ is a $K \times K$ circulant matrix with $\bar{\mathbf{c}}_{r,q} \triangleq [c_r(q,0), c_r(q,1), \ldots, c_r(q,L-1), \mathbf{0}_{1\times(K-L)}]^T$ as its first column; and $\mathbf{0}_{1\times(K-L)}$ denotes the $1 \times (K-L)$ all-zero vector.

By substituting (38) into (2), we then obtain

$$\mathbf{y}_r = \mathbf{F}\tilde{\mathbf{H}}_r\mathbf{F}^H\mathbf{x} + \mathbf{n}_r \tag{39}$$

$$= \mathbf{F}\sum_{q=0}^{Q}\tilde{\mathbf{D}}_q\mathbf{G}_{r,q}\mathbf{F}^H\mathbf{x} + \mathbf{n}_r \tag{40}$$

$$= \mathbf{F}\sum_{q=0}^{Q}\tilde{\mathbf{D}}_q\mathbf{F}^H\mathbf{F}\mathbf{G}_{r,q}\mathbf{F}^H\mathbf{x} + \mathbf{n}_r. \tag{41}$$

Note that, if $\mathbf{G}_{r,q}$ is a circulant matrix with $\bar{\mathbf{c}}_{r,q}$ as its first column, then $\bar{\mathbf{G}}_{r,q} \triangleq \mathbf{F}\mathbf{G}_{r,q}\mathbf{F}^H$ is a diagonal matrix with $\sqrt{K}\mathbf{F}\bar{\mathbf{c}}_{r,q}$ on its diagonal [32].

Then, (41) can be further represented as

$$\mathbf{y}_r = \mathbf{F}\sum_{q=0}^{Q}\mathrm{diag}\{\mathbf{b}_q\}\mathbf{F}^H\mathrm{diag}\left\{\sqrt{K}\mathbf{F}\bar{\mathbf{c}}_{r,q}\right\}\mathbf{x} + \mathbf{n}_r \tag{42}$$

$$= \sum_{q=0}^{Q}\mathbf{F}\,\mathrm{diag}\{\mathbf{b}_q\}\mathbf{F}^H\mathrm{diag}\{\mathbf{F}_L\mathbf{c}_{r,q}\}\mathbf{x} + \mathbf{n}_r \tag{43}$$

where it is easy to have $\mathbf{F}\bar{\mathbf{c}}_{r,q} = (1/\sqrt{K})\mathbf{F}_L\mathbf{c}_{r,q}$ with $\mathbf{c}_{r,q} \triangleq [c_r(q,0), \ldots, c_r(q,L-1)]^T$, and $\mathbf{F}_L$ denotes the first L columns of $\sqrt{K}\mathbf{F}$. Hence, we can finally have (8).

REFERENCES

[1] Y. Mostofi and D. Cox, "ICI mitigation for pilot-aided OFDM mobile systems," *IEEE Trans. Wireless Commun.*, vol. 4, no. 2, pp. 765–774, Mar. 2005.

[2] K. Kwak, S. Lee, H. Min, S. Choi, and D. Hong, "New OFDM channel estimation with dual-ICI cancellation in highly mobile channel," *IEEE Trans. Wireless Commun.*, vol. 9, no. 10, pp. 3155–3165, Oct. 2010.

[3] Z. Tang, R. Cannizzaro, G. Leus, and P. Banelli, "Pilot-assisted time-varying channel estimation for OFDM systems," *IEEE Trans. Signal Process.*, vol. 55, no. 5, pp. 2226–2238, May 2007.

[4] X. Ma, G. Giannakis, and S. Ohno, "Optimal training for block transmissions over doubly-selective wireless fading channels," *IEEE Trans. Signal Process.*, vol. 51, no. 5, pp. 1351–1366, May 2003.

[5] W. Bajwa, A. Sayeed, and R. Nowak. "Sparse multipath channels: Modeling and estimation," in *Proc. IEEE Digit. Signal Process. Educ. Workshop*, Jan. 2009, pp. 320–325.

[6] W. Bajwa, J. Haupt, A. Sayeed, and R. Nowak, "Compressed channel sensing: A new approach to estimating sparse multipath channels," *Proc. IEEE*, vol. 98, no. 6, pp. 1058–1076, Jun. 2010.

[7] W. Bajwa, A. Sayeed, and R. Nowak, "Learning sparse doubly-selective channels," in *Proc. 46th Annu. Allerton Conf. Commun., Control Comput.*, Sep. 2008, pp. 575–582.

[8] G. Gui, W. Peng, and F. Adachi, "High-resolution compressive channel estimation for broadband wireless communication systems," *Int. J. Commun. Syst.*, vol. 27, no. 10, pp. 2396–2407, Dec. 2014.

[9] G. Gui, L. Xu, L. Shan, and F. Adachi, "Compressive sensing based Bayesian sparse channel estimation for OFDM communication systems: High performance and low complexity," *Sci. World J.*, vol. 2014, 2014, Art. ID. 927 894.

[10] G. Gui and F. Adachi, "Improved adaptive sparse channel estimation using least mean square algorithm," *EURASIP J. Wireless Commun. Netw.*, vol. 2013, no. 1, pp. 1–18, Aug. 2013.

[11] G. Taubock, F. Hlawatsch, D. Eiwen, and H. Rauhut, "Compressive estimation of doubly selective channels in multicarrier systems: Leakage effects and sparsity-enhancing processing," *IEEE J. Sel. Topics Signal Process.*, vol. 4, no. 2, pp. 255–271, Apr. 2010.

[12] D. Donoho, M. Elad, and V. Temlyakov, "Stable recovery of sparse overcomplete representations in the presence of noise," *IEEE Trans. Inf. Theory*, vol. 52, no. 1, pp. 6–18, Jan. 2006.

[13] E. Candes, J. Romberg, and T. Tao, "Robust uncertainty principles: Exact signal reconstruction from highly incomplete frequency information," *IEEE Trans. Inf. Theory*, vol. 52, no. 2, pp. 489–509, Feb. 2006.

[14] M. Elad, "Optimized projections for compressed sensing," *IEEE Trans. Signal Process.*, vol. 55, no. 12, pp. 5695–5702, Dec. 2007.

[15] X. He and R. Song, "Pilot pattern optimization for compressed sensing based sparse channel estimation in OFDM systems," in *Proc. Int. Conf. WCSP*, Oct. 2010, pp. 1–5.

[16] C. Qi and L. Wu, "Optimized pilot placement for sparse channel estimation in OFDM systems," *IEEE Signal Process. Lett.*, vol. 18, no. 12, pp. 749–752, Dec. 2011.

[17] X. Ren, W. Chen, and Z. Wang, "Low coherence compressed channel estimation for high mobility MIMO OFDM systems," in *Proc. IEEE GLOBECOM*, Dec. 2013, pp. 3389–3393.

[18] X. Ren, W. Chen, and M. Tao, "Position-based compressed channel estimation and pilot design for high-mobility OFDM systems," *IEEE Trans. Veh. Technol.*, vol. 64, no. 5, pp. 1918–1929, Jul. 2014.

[19] P. Cheng *et al.*, "Channel estimation for OFDM systems over doubly selective channels: A distributed compressive sensing based approach," *IEEE Trans. Commun.*, vol. 61, no. 10, pp. 4173–4185, Oct. 2013.

[20] F. Campos, R. Alvarez, O. Gandara, and R. Michel, "Estimation of fast time-varying channels in OFDM systems using two-dimensional prolate," *IEEE Trans. Wireless Commun.*, vol. 12, no. 2, pp. 898–907, Feb. 2013.

[21] E. Simon *et al.*, "Joint carrier frequency offset and fast time-varying channel estimation for MIMO-OFDM systems," *IEEE Trans. Veh. Technol.*, vol. 60, no. 3, pp. 985–965, Mar. 2011.

[22] E. Simon, L. Ros, H. Hijazi, and M. Ghogho, "Joint carrier frequency offset and channel estimation for OFDM systems via the EM algorithm in the presence of very high mobility," *IEEE Trans. Signal Process.*, vol. 60, no. 2, pp. 754–765, Feb. 2012.

[23] L. Liu *et al.*, "Position-based modeling for wireless channel on high-speed railway under a viaduct at 2.35 GHz," *IEEE J. Sel. Areas Commun.*, vol. 30, no. 4, pp. 834–845, May 2012.

[24] R. Pascoe and T. Eichorn, "What is communication-based train control?" *IEEE Veh. Technol. Mag.*, vol. 4, no. 4, pp. 16–21, Dec. 2009.

[25] A. Kannu and P. Schniter, "MSE-optimal training for linear time-varying channels," in *Proc. IEEE ICASSP*, Mar. 2005, pp. 789–792.

[26] G. Leus, "On the estimation of rapidly time-varying channels," in *Proc. EUSIPCO*, Sep. 2004, pp. 2227–2230.

[27] D. Borah and B. Hart, "Frequency-selective fading channel estimation with a polynomial time-varying channel model," *IEEE Trans. Commun.*, vol. 47, no. 6, pp. 862–873, Jun. 1999.

[28] T. Zemen and C. Mecklenbräuker, "Time-variant channel estimation using discrete prolate spheroidal sequences," *IEEE Trans. Signal Process.*, vol. 53, no. 9, pp. 3597–3607, Sep. 2005.

[29] E. Candes and M. Wakin, "An introduction to compressive sampling," *IEEE Signal Process. Mag.*, vol. 25, no. 2, pp. 21–30, Mar. 2008.

[30] S. Chen, D. Donoho, and M. Saunders, "Atomic decompostiion by basis pursuit," *SIAM Rev.*, vol. 43, no. 1, pp. 129–159, 2001.

[31] Y. Pati, R. Rezaiifar, and P. Krishnaprasad, "Orthogonal matching pursuit: Recursive function approximation with applications to wavelet decomposition," in *Proc. 27th Annu. Asilomar Conf. Signals, Syst. Comput.*, Nov. 1993, vol. 1, pp. 40–44.

[32] F. Hlawatsch and G. Matz, *Wireless Communications Over Rapidly Time-Varying Channels.* New York, NY, USA: Academic, 2011.

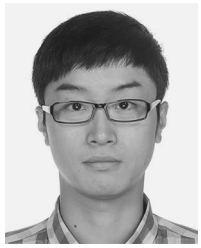

Xiang Ren received the B.S. degree in electronic engineering from Wuhan University, Wuhan, China, in 2011. He is currently working toward the Ph.D. degree with Network Coding and Transmission Laboratory, Shanghai Jiao Tong University, Shanghai, China.

His current research interests include channel estimation, high-mobility channels, and multiple-input–multiple-output orthogonal frequency-division multiplexing systems.

Meixia Tao (S'00–M'04–SM'10) received the B.S. degree in electronic engineering from Fudan University, Shanghai, China, in 1999 and the Ph.D. degree in electrical and electronic engineering from Hong Kong University of Science and Technology, Hong Kong, in 2003.

From 2003 to 2004, she was a member of the Professional Staff with the Hong Kong Applied Science and Technology Research Institute. From 2004 to 2007, he was a Teaching Fellow and then an Assistant Professor with the Department of Electrical and Computer Engineering, National University of Singapore, Singapore. She is currently a Professor with the Department of Electronic Engineering, Shanghai Jiao Tong University. Her current research interests include cooperative communications, wireless resource allocation, multiple-input–multiple-output techniques, and physical-layer security.

Dr. Tao has been a member of the Executive Editorial Committee of the IEEE TRANSACTIONS ON WIRELESS COMMUNICATIONS since January 2015. She was on the Editorial Board of the IEEE TRANSACTIONS ON WIRELESS COMMUNICATIONS from 2007 to 2011 and the IEEE COMMUNICATIONS LETTERS from 2009 to 2012. She serves as an Editor for IEEE TRANSACTIONS ON COMMUNICATIONS and IEEE WIRELESS COMMUNICATIONS LETTERS. She also served as a Guest Editor for IEEE COMMUNICATIONS MAGAZINE with the featured topic Long-Term Evolution Advanced and fourth-generation wireless communications in 2012 and for *EURASIP Journal on Wireless Communications and Networking* special issue on physical-layer network coding for wireless cooperative networks in 2010. She served as the Technical Program Committee Chair for the IEEE/CIC International Conference on Communications in China in 2014 and as a Symposium Cochair for the IEEE International Conference on Communications in 2015. She received the IEEE Heinrich Hertz Award for Best Communications Letters in 2013, the IEEE Communication Society Asia–Pacific Outstanding Young Researcher Award in 2009, and the International Conference on Wireless Communications and Signal Processing Best Paper Award in 2012.

Wen Chen (M'03–SM'11) received the B.S. and M.S. degrees from Wuhan University, Hubei, China, in 1990 and 1993, respectively, and the Ph.D. degree from the University of Electro-Communications, Tokyo, Japan, in 1999.

From 1999 to 2001, he was a Researcher with the Japan Society for the Promotion of Sciences. In 2001, he joined the University of Alberta, Edmonton, AB, Canada, starting as a Postdoctoral Fellow with the Information Research Laboratory and continuing as a Research Associate with the Department of Electrical and Computer Engineering. Since 2006, he has been a Full Professor with the Department of Electronic Engineering, Shanghai Jiao Tong University, Shanghai, China, where he is also the Director of the Institute for Signal Processing and Systems. His research interests include network coding, cooperative communications, cognitive radio, and multiple-input–multiple-output orthogonal frequency-division multiplexing systems.